11106–11120 *Nucleic Acids Research, 2017, Vol. 45, No. 19* *Published online 21 August 2017*
doi: 10.1093/nar/gkx727

The PRMT5/WDR77 complex regulates alternative splicing through ZNF326 in breast cancer

Madhumitha Rengasamy[1,2], Fan Zhang[3,4], Ajay Vashisht[5], Won-Min Song[2], Francesca Aguilo[6], Yifei Sun[1,2,7], SiDe Li[1,7], Weijia Zhang[3], Bin Zhang[2], James A. Wohlschlegel[5] and Martin J. Walsh[1,2,7,*]

[1]Department of Pharmacological Sciences, Icahn School of Medicine at Mount Sinai, New York, NY 10029, USA, [2]Department of Genetics and Genomic Sciences, Icahn School of Medicine at Mount Sinai, New York, NY 10029, USA, [3]Department of Medicine, Division of Nephrology, Bioinformatics Laboratory, Icahn School of Medicine at Mount Sinai, New York, NY 10029, USA, [4]Center for Life Sciences, School of Life Sciences and Technology, Harbin Institute of Technology, Harbin 150080, China, [5]Departmentof Biological Chemistry and the Institute of Genomics and Proteomics, University of California, Los Angeles, CA 90095, USA, [6]Wallenberg Centre for Molecular Medicine, Department of Medical Biosciences, University of Umeå, Försörjningsvägen 19073, Umeå, Sweden and [7]The Mount Sinai Center for RNA Biology and Medicine, Icahn School of Medicine at Mount Sinai, New York, NY 10029, USA

Received July 21, 2017; Editorial Decision August 07, 2017; Accepted August 11, 2017

ABSTRACT

We observed overexpression and increased intranuclear accumulation of the PRMT5/WDR77 in breast cancer cell lines relative to immortalized breast epithelial cells. Utilizing mass spectrometry and biochemistry approaches we identified the Zn-finger protein ZNF326, as a novel interaction partner and substrate of the nuclear PRMT5/WDR77 complex. ZNF326 is symmetrically dimethylated at arginine 175 (R175) and this modification is lost in a *PRMT5* and *WDR77*-dependent manner. Loss of *PRMT5* or *WDR77* in MDA-MB-231 cells leads to defects in alternative splicing, including inclusion of A-T rich exons in target genes, a phenomenon that has previously been observed upon loss of *ZNF326*. We observed that the alternatively spliced transcripts of a subset of these genes, involved in proliferation and tumor cell migration like *REPIN1*/*AP4*, *ST3GAL6*, *TRNAU1AP* and *PFKM* are degraded upon loss of PRMT5. In summary, we have identified a novel mechanism through which the PRMT5/WDR77 complex maintains the balance between splicing and mRNA stability through methylation of ZNF326.

INTRODUCTION

Protein arginine methyltransferases (PRMTs) are a family of enzymes that catalyze the transfer of a methyl group from the co-factor S-adenosyl-l-methionine (AdoMet) to a variety of substrates including histones (1) and transcription factors (2,3). PRMTs can be classified into three types—Type I, which includes PRMTs 1–4,6 and 8, catalyze the formation of asymmetric dimethylarginines; Type II, which includes PRMT5 and PRMT9 (4), catalyze the formation of symmetric dimethylarginines and Type III, the sole member of which is PRMT7, catalyzes the formation of monomethylarginines (3). PRMT5 is the predominant Type II methyltransferase and is found in a tight hetero-octameric complex with its substrate-binding partner WDR77 (or MEP50) (5,6). Along with pICln, PRMT5 and WDR77 form the 20S methylosome in the cytoplasm, symmetrically dimethylating spliceosome proteins prior to their assembly (7). Apart from spliceosome proteins, the PRMT5/WDR77 complex also symmetrically dimethylates several proteins, including histones (8,9), transcription factors (10–13) and chromatin remodeling factors (14). Loss of PRMT5 leads to severe defects in constitutive and alternative splicing that has been attributed to the loss in methylation of spliceosome proteins (15,16). Moreover, studies have implicated the role of *prmt5* within an *Arabidopsis thaliana* model for circadian period determination to the global regulation of altered splicing where patterns distinctly favour effective splicing of *period* and other *clock*-related genes (17,18).

However, little work has been done to understand if the PRMT5/WDR77 complex has a 20S methylosome independent role in regulating splicing. PRMT5 and WDR77 are overexpressed in several types of cancer including lung (19), brain (20), lymph (21), prostate (22), ovarian (23) and breast (24). In breast and ovarian cancer, the com-

*To whom correspondence should be addressed. Tel: +1 212 241 9714; Fax: +1 212 996 7214; Email: martin.walsh@mssm.edu
Present address: Martin J. Walsh, Ph.D. The Mount Sinai Center for RNA Biology and Medicine, Departments of Pharmacological Sciences, Genetics and Genomic Sciences, Icahn School of Medicine at Mount Sinai, 1468 Madison Ave., Box 1656, New York, NY 10029, USA.

plex shows increased intra-nuclear accumulation (23,24) making it an ideal model system to understand if the PRMT5/WDR77 complex has a 20S methylosome independent role in regulating splicing. We characterized the protein interactome of WDR77 in the estrogen receptor negative (ER-) breast cancer cell line MDA-MB-231, and identified ZNF326 as a novel interaction partner and substrate of the PRMT5/WDR77 complex. RNA-seq analysis revealed global defects in alternative splicing upon loss of PRMT5 and WDR77. Interestingly, loss of PRMT5 and WDR77 leads to inclusion of AT-rich exons at target genes, a phenomenon previously observed upon loss of ZNF326. We also observed that a subset of these alternatively spliced transcripts including *AP4*, *ST3GAL6* and *TRNAU1AP* are also downregulated upon loss of PRMT5. Collectively, we have identified a previously uncharacterized role of the PRMT5/WDR77 complex in regulating alternative splicing and shaping the transcriptome of breast cancer cells.

MATERIALS AND METHODS

Cell culture

MDA-MB-231 cells were obtained from ATCC and cultured in Dulbecco's modified essential medium (DMEM) containing 10% fetal bovine serum (FBS) and passaged one or two times a week. MCF10A cells were a kind gift from Dr Doris Germain. MCF10A cells were grown in DMEM/F12 media containing 5% horse serum, 0.02 mg/ml epithelial growth factor, 0.5 μg/ml hydrocortisone, 0.1 μg/ml cholera toxin, 0.01 mg/ml of insulin and 1% Penicillin-Streptomycin. MCF7 cells were obtained from ATCC and cultured in DMEM containing 10% FBS. T47D cells were obtained from ATCC and cultured in Roswell Park Memorial Institute (RPMI) 1640 medium containing 10% FBS. HCC38 cells were a kind gift from Dr Stuart Aaronson. HCC38 cells were cultured in RPMI medium containing 10% FBS. All cell lines used within this study were first authenticated by short tandem repeats profiling through (American Type Tissue Collection, ATCC). Cells were maintained in mycoplasma-free conditions; however, all cultures were tested after every other passage for mycoplasma contamination.

Preparation of nuclear and cytoplasmic extracts

Cells were expanded to 150 mm diameter tissue culture plates, washed with cold phosphate-buffered saline and detached using a cell scraper and transferred to 15 ml tubes. The tubes were spun down at 200 *g* for 5 min. The cell pellet was resuspended in at least five volumes of buffer A (10 mM HEPES pH 7.9, 1.5 mM MgCl2, 10 mM KCl, 1 mM Dithiothreitol (DTT)) in the presence of protease inhibitors (Roche) and incubated for 10 min on ice. The cell suspension was spun down at 500 *g* for 10 min. Following centrifugation; the pellet was resuspended in two volumes of buffer A, Douncer-homogenized and then spun down at 25,127 *g* for 20 min at 4°C.

The supernatant was used as the cytoplasmic fraction. The pellet (nuclei) was resuspended in 0.75 ml of salt-free Buffer C per ml of original pellet (**20 mM HEPES pH 7.9, 1.5 mM MgCl2, 25% Glycerol, 0.5 mM ethylenediaminetetraacetic acid (EDTA), 1 mM DTT) supplemented with protease inhibitors. A total of 22.86 μl of 5M NaCl was added per ml of the original pellet followed by two strokes of the Dounce homogenizer. This step was repeated for six more times till the salt concentration reached 0.4M NaCl. The nuclear lysate was then transferred to microfuge tubes and incubated on a rotator at 4°C for 30 min. Finally, the samples were spun down at maximum speed for 1 h at 4°C. The protein concentration was estimated using the Bradford assay and the nuclear and cytoplasmic extracts were flash frozen and stored at −80°C until use.

Co-immunoprecipitation and immunoblotting

For immunoprecipitation, 200 μg of nuclear extracts were first pre-cleared with protein G Dynabeads (Invitrogen) for 1 h at 4°C. The pre-cleared extracts were incubated overnight with 2–3 μg of antibody at 4°C on a rocker. The next day, the extracts were incubated with Protein G Dynabeads for 2 h and then the conjugated beads were washed four times in ice-cold Nonidet P-40 buffer (20 mM Tris HCl pH 8, 137 mM NaCl, 1% Nonidet P-40 (NP-40), 2 mM EDTA) supplemented with protease inhibitors (Roche). Immunoprecipitated complexes were resolved by sodium dodecyl sulphate-polyacrylamide gel electrophoresis (SDS-PAGE), transferred to nitrocellulose membranes (Bio-Rad), and immunoblotted with the indicated antibodies followed by ECL detection (Thermo Scientific).

LC-MS/MS to identify WDR77 interacting proteins

Eight micrograms (8ug) of WDR77 antibody were conjugated to 0.5 mg of Dynabeads® M-270 Epoxy according to the manufacture's instructions (Invitrogen). Then, 1 mg of nuclear and cytoplasmic extracts were incubated with antibody-coupled beads overnight at 4°C. After washing four times with NP40 buffer, immunoprecipitated complexes were eluted with 100 μl of 100 mM Glycine buffer (pH 2.2) for 10 min at RT and neutralized by adding 1/10 volume of 1M Tris–HCl (pH 8.0).

Liquid chromatography followed by tandem mass spectrometry (LC-MS/MS) was performed and data analyzed by Dr Ajay Vashisht and Dr James Wohlschlegel at the University of California, Los Angeles. The immunopurified protein complexes were reduced, alkylated and digested by sequential addition of endopeptidase lys-C and trypsin as described (25,26). The digested peptide mixture was first desalted, concentrated and fractionated online using a 75 μM inner diameter fritted fused silica capillary column, with a 5 μM pulled electrospray tip and packed in-house with 15 cm of Luna C18 (2) 3 μM reversed phase particles. The gradient was delivered by an easy-nLC 1000 ultra high-pressure liquid chromatography (UHPLC) system (Thermo Scientific). MS/MS spectra were collected on a Q-Exactive mass spectrometer (Thermo Scientific) (27,28). Data analysis was performed using the ProLuCID and DTASelect2 implemented in the Integrated Proteomics Pipeline—IP2 (Integrated Proteomics Applications, Inc., San Diego, CA, USA) (29–32). Protein and peptide identifications were filtered using DTASelect, required at least two unique peptides per

protein and a peptide-level false positive rate of 5% as estimated by a decoy database strategy (33). Normalized spectral abundance factor (NSAF) values were calculated as described (34). For the ease of readability NSAF values were multiplied by a factor of 10^5.

Identification of methylated arginine residue on ZNF326 by tandem mass spectrometry

Endogenous ZNF326 was immunopurified from scrambled and PRMT5 shRNA transfected cells. The immunopurified ZNF326 was analyzed by SDS-PAGE and the region of gel corresponding to ZNF326 molecular weight was excised, digested in the excised gel slices using trypsin, and analyzed by mass spectrometry as described on a Thermofisher Q-Exactive tandem mass spectrometer (25,27,28). Data analysis was performed using the ProLuCID and DTASelect2 algorithms as implemented in the Integrated Proteomics Pipeline—IP2 (Integrated Proteomics Applications, Inc., San Diego, CA, USA) (30,31). Dimethylated peptides were identified using a differential modification search that considered a mass shift of +28.0314 on arginine residue. All peptide-spectrum matches were evaluated by DTASelect2 and filtered using maximum false detection rate of 5% using a decoy database approach (33). Label-free quantitation of the peptides was performed using the Skyline software package (35). Peak evaluation was carried out through manual interrogation of the data (35,36). For all the peptides corresponding to ZNF326, peak areas were added for three isotopic peaks (M, M+1, M+2) to serve as the peptide's quantitative measure. Relative peptide abundance for modified and unmodified peptides were calculated from respective peak areas exported from Skyline from scrambled and PRMT5 shRNA samples.

Generation of lentiviruses

pLKO-based shRNAs targeting PRMT5 and WDR77 and a scrambled control were purchased from Sigma. Lentiviruses were generated in HEK-293T cells by Superfect-mediated cotransfection of lentiviral-based shRNA plasmids and the pCMV-dR8.2 (packaging) and pCMV-VSVG (envelope) plasmids. Viral supernatants were concentrated using Amicon Ultra centrifugal filter units (Millipore) at 1600 *g* for 20 min and stored in aliquots at −80°C.

Infection of MDA-MB-231 cells with lentiviruses

For infection, MDA-MB-231 cells were transduced with virus in serum free DMEM. Cells were incubated overnight with virus and subsequently cultured in fresh media. Seventy-two hours after infection the cells were cultured in media supplemented with 1 μg/ml puromycin. The cells were harvested on the 10th day after infection for cell viability/apoptosis assays, RNA and protein extraction.

RT-PCR

RNA was extracted using the RNeasy kit from Qiagen. cDNA was prepared using 1–2 μg of RNA using PrimeScript First Strand cDNA Synthesis Kit from Takara Biosciences. Quantitative polymerase chain reaction (qPCR) was performed using the GoTaq® qPCR Master Mix (Promega) on the Stratagene Mx3005P Real-Time PCR System (Agilent Technologies) using 15–20 ng of cDNA per reaction. Primers used are listed in Supplementary Table 4. To calculate inclusion/exclusion of exons $\log_2$ fold change values were calculated. The $\log_2$ fold change for gene expression was subtracted from the included/excluded exons values to account for downregulation of gene expression.

Library preparation for RNA-seq

Library preparation for RNA-seq analysis was performed by the Weill Cornell Medical College Genomic Core facility (New York, NY, USA) using the TrueSeq RNA sample preparation kit (Illumina RS-22–2001) as per manufacturer's recommendations. Samples were sequenced by the Illumina HiSeq 2500 platform (Illumina) as 100 bp pair-ended reads.

RNA-seq analysis

After filtering contaminant (aligned) reads, the reads with good quality were aligned to several human reference databases including hg19 genome, RefSeq exons, splicing junctions using the Burrows-Wheeler Aligner (BWA) algorithm (37). The reads that were uniquely aligned to the exon and splicing-junction sites for each transcript were then counted as expression level for a corresponding transcript and were subjected to $\log_2$ transformation and global median normalization, to compare transcripts levels among distinct samples. Differentially expressed genes were identified by the R package DEGseq (38) using a false discovery rate < 0.001 and fold-change > 1.5. Gene ontology analysis was performed using DAVID (39,40).

Statistical analysis

All values were expressed as mean ± SD. Statistical analysis was performed by the Paired Student's *t*-test. A probability value of $P < 0.05$ was considered statistically significant.

Antibodies

The following commercially available antibodies were used at the indicated concentrations for western blot: anti–β-actin (Sigma, A5441, 1:1,000), anti-WDR77 (Bethyl, A301–562A, 1:1,000), anti-PRMT5 (Bethyl, A300–850A, 1:1,000), anti-ZNF326 (Bethyl, A301–880A, 1:1,000), anti-HNRNPH1 (Bethyl, A300–511A, 1:1,000) Anti-dimethyl-Arginine, symmetric (SYM10) (Millipore, 07–412, 1:1000), Anti-Histone H3 antibody (Abcam, ab1791, 1:1000), Anti-Histone H4 (symmetric di methyl R3) (ab5823, 1:1000), Anti-Histone H2A (symmetric di methyl R3) antibody (Abcam,ab22397, 1:1000).

The following antibodies were used for co-immunoprecipitation: Rabbit Control IgG (Abcam, ab46540), anti-PRMT5 (Bethyl, A300–849A). For ZNF326 and WDR77 the same antibodies were used for western blot and immunoprecipitation.

RESULTS

PRMT5 and WDR77 show nuclear localization in MDA-MB-231 cells and are essential for cell survival

To analyze the expression of PRMT5 and WDR77 in breast cancer we performed in silico analysis of the The Cancer Genome Atlas (TCGA) database. We identified over-expression of WDR77 ($P = 7.5 \times 10^{-7}$) and PRMT5 ($P = 2.07 \times 10^{-3}$) in breast tumor samples relative to matched normal samples ($n = 109$) (Figure 1A). We verified this observation by qPCR with reverse transcription (RT-qPCR) analysis (Figure 1B) of immortalized breast epithelial (MCF10A), estrogen receptor negative (ER-: MDA-MB-231, HCC38) and estrogen receptor positive (ER+: T47D and MCF7) breast cancer cell lines. We observed significant over-expression of WDR77 (HCC38) or PRMT5 (MCF7) or both (MDA-MB-231 and T47D) in the breast cancer cell lines relative to immortalized breast epithelial cells (MCF10A).

In agreement with these findings, western blots of nuclear and cytoplasmic extracts of the cell lines showed increased nuclear accumulation of WDR77 (MCF7, MDA-MB-231 and T47D) and PRMT5 (MCF7 and MDA-MB-231) in breast cancer cell lines relative to MCF10A (Figure 1C). We ascertained the purity of nuclear and cytoplasmic fractions by immunoblotting for histone H3 and α-tubulin respectively (Supplementary Figure S1A and B).

T47D showed increased expression of *PRMT5* transcript but not protein compared to MCF10A cells (Figures 1B and C) suggesting post-transcriptional regulation of the *PRMT5* transcript. miR92b/96 has been shown to regulate *PRMT5* translation in mantle cell lymphoma (21). It is possible that there might be increased expression of miR92b/96 in T47D causing translational repression of the PRMT5 transcript. On the other hand MCF7 does not show increased expression of *WDR77* transcript but there is increase in WDR77 protein (Figures 1B and C) suggesting increased stability of the WDR77 transcript. Interestingly, WDR77 has a long 3′UTR (1340 nt) but to date there have been no studies to explore its post-transcriptional regulation by repressor proteins or miRNA.

Several papers have reported the role of WDR77 as an androgen and estrogen receptor co-factor (23,41). To understand the estrogen-receptor-independent role of the PRMT5/WDR77 complex and to eliminate complications arising from estrogen receptor-mediated changes in chromatin structure and gene expression (42,43) we chose to study the mechanism of oncogenesis mediated by the PRMT5/WDR77 complex in an ER- cell line. We chose the triple-negative, invasive breast cancer cell line MDA-MB-231, to characterize the role of nuclear PRMT5/WDR77 complex in mediating oncogenesis.

To investigate the tumor-promoting activity of the PRMT5/WDR77 complex, we performed lentiviral-mediated short hairpin RNA (shRNAs) (listed in Supplementary Table S1) depletion of *WDR77* and *PRMT5* in MDA-MB-231 cells (Figure 1D). Loss of WDR77 or PRMT5 resulted in destabilization of the partner protein (Figure 1E) in line with previous observations (44,45) highlighting the interdependence of these proteins for stability. Surprisingly, loss of PRMT5 also caused transcriptional downregulation of WDR77 (Figure 1D and E). We showed for the first time the multi-layered regulation of WDR77 by PRMT5, both at the level of mRNA transcript (either through transcriptional or post-transcriptional regulation) and protein. Loss of PRMT5, but not WDR77, led to loss in global levels of the symmetrically dimethylated histone marks H2AR3Me2s, H4R3Me2s and H3R2Me2s (Supplementary Figure S1C) suggesting that residual levels of PRMT5 remaining upon loss of WDR77 was sufficient to catalyze histone modifications. Loss of WDR77 and PRMT5 resulted in reduced cell viability (Supplementary Figure S1D) and apoptosis (Figure 1F) recapitulating previous observations (15,46,47) underscoring the importance of these proteins for cell survival.

WDR77 interacts with novel proteins involved in RNA processing and splicing

Apart from the spliceosome proteins (7) and histones (48), the PRMT5/WDR77 complex interacts with several proteins including SKI (8), CYCLIN D1/CDK4 (49) and TP53 (10). However there has been no comprehensive analysis of the repertoire of interaction partners for the PRMT5/WDR77 complex.

In order to characterize the endogenous interaction partners of this complex, we immunoprecipitated the substrate binding partner, WDR77, from nuclear and cytoplasmic extracts of MDA-MB-231 cells (Supplementary Figure S2A and B) and analyzed it by LC-MS/MS. We identified a total of 97 and 90 interaction partners of WDR77 from the cytoplasm and nucleus respectively (Supplementary Tables S2 and 3). The most enriched interaction partners of WDR77 were common between the nucleus and cytoplasm highlighting the shuttling nature of this complex (Supplementary Figure S2C).

We identified WDR77 (bait) and PRMT5, as well as peptides representative of small nuclear ribonucleoproteins (SNRNP's) RIOK1, and CLNS1A, consistent with previously reported binding partners of WDR77 (7) (50) thus validating our approach.

We identified several novel interaction partners of WDR77 in the cytoplasm and nucleus. mRNA metabolism, translation and co-translational targeting of proteins were the biological pathways enriched among the cytoplasmic interaction partners of WDR77 (Figure 2A). Network analysis of the most enriched proteins revealed novel interacting partners involved in RNA processing and splicing (HNRNP H1 and H2), RNA stability (SERBP1), translation (RPS27A, RPS3, RPS10L) and protein folding (CCT7) (Figure 2B). The nuclear interaction partners of WDR77 were enriched for biological pathways involved in RNA metabolism, processing and splicing (Figure 2C). Among the top novel interaction partners in the nucleus were proteins involved in splicing (HNRNP H1 and H2, ZNF326), RNA stability (SERBP1), translation (RPS27A, RPL26) and sterol synthesis (OSBP) (Figure 2D).

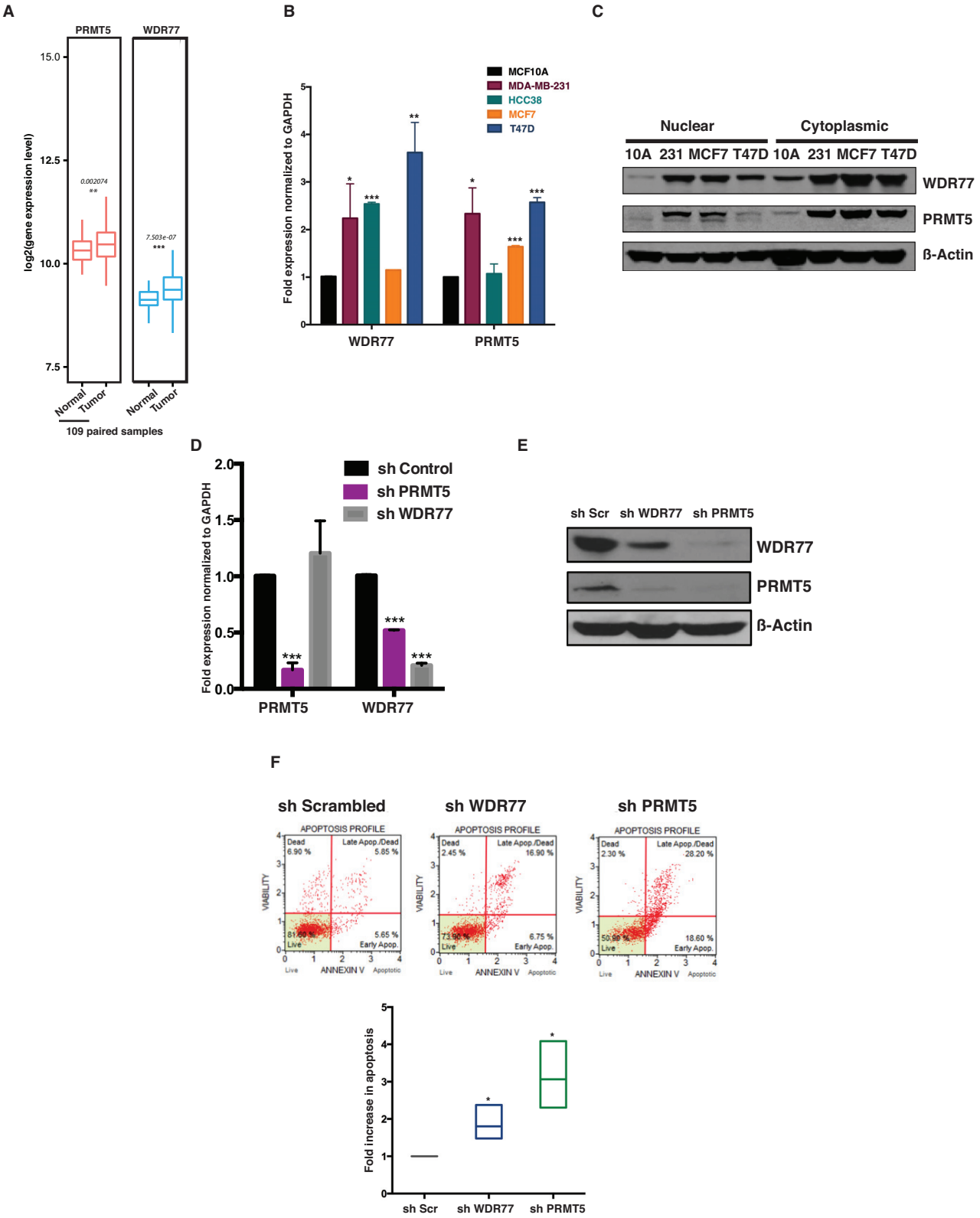

Figure 1. Expression of *PRMT5* and *WDR77* in breast cancer (**A**). Expression analysis of 109 paired samples from The Cancer Genome Atlas (TCGA) database shows significant overexpression of PRMT5 and WDR77 in breast cancer samples relative to matched normal samples (**B**). Fold expression of WDR77 and PRMT5 in breast normal (MCF10A), ER+ (MCF7, T47D) and ER- (MDA-MB-231, HCC38) breast cancer cell lines. Normalized to GAPDH (**C**). Immunoblotting of WDR77 and PRMT5 in nuclear and cytoplasmic extracts of breast normal and cancer cell lines. Actin was used as loading control. (**D**). Fold expression (relative to GAPDH) of *WDR77* and *PRMT5* and (**E**). Immunoblotting of the respective proteins in sh Scrambled, sh WDR77 and sh PRMT5-treated samples. Actin was used as loading control in E (**F**). (Top panel) Annexin V staining showing increased number of apoptotic cells upon loss of *WDR77* and *PRMT5*. (Bottom panel) Box plots of results from apoptosis assay for three biological replicates. Student's t-test $*P < 0.05$ $**P < 0.005$ $***P < 0.0005$.

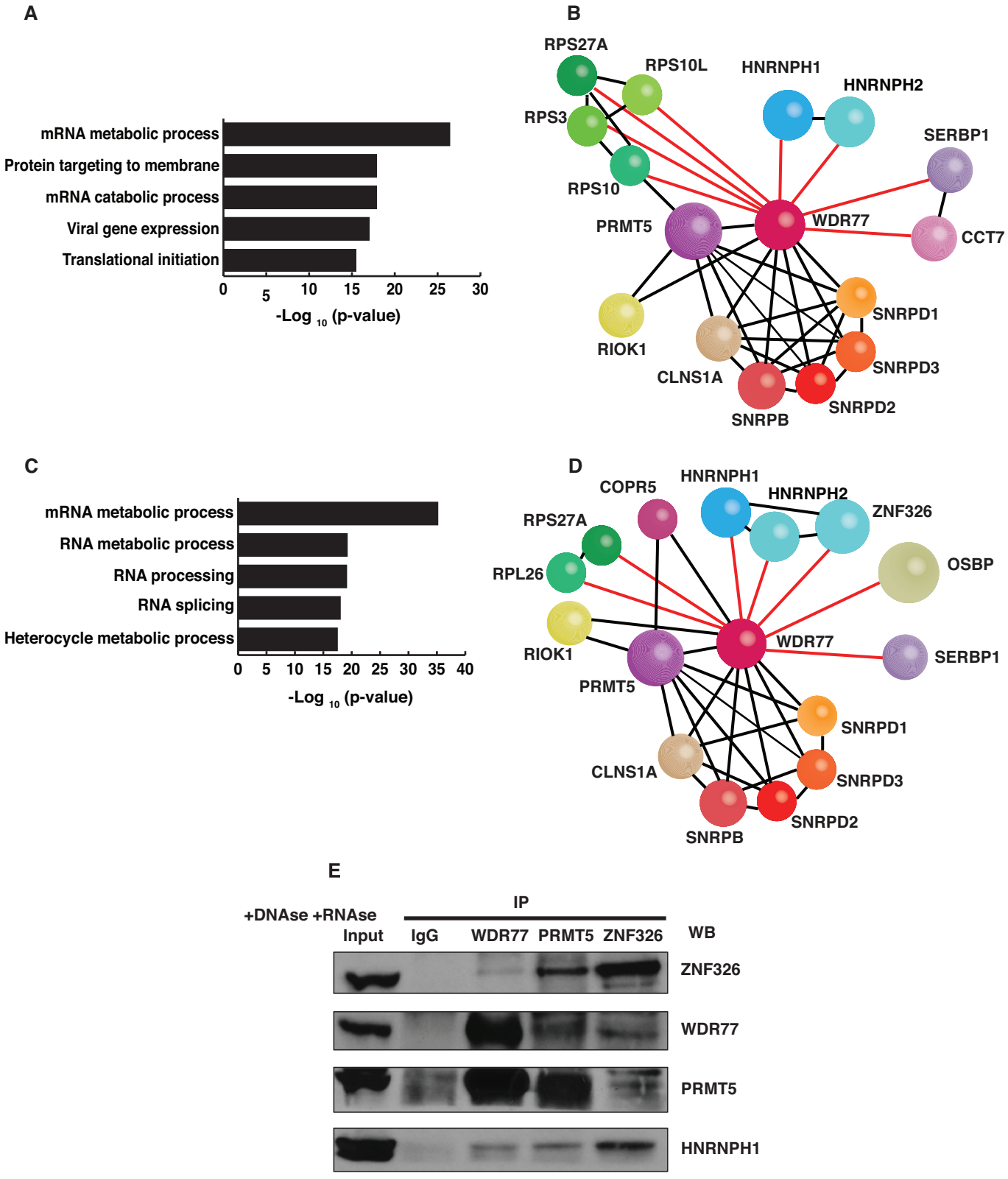

Figure 2. Networks of top interaction partners of WDR77 in the cytoplasm and nucleus identified by LC-MS/MS (**A**). Gene ontology analysis (**B**). Protein interaction network of top 15 interacting partners of WDR77 in the cytoplasm (red lines: newly identified interactions, black lines: previously characterized interactions) (**C**). Gene ontology analysis (**D**). Protein interaction network of top 15 interacting partners of WDR77 in the nucleus (red lines: newly identified interactions, black lines: previously characterized interactions) (**E**). Immunoblots of co-immunoprecipitations of WDR77, PRMT5 and ZNF326 (IP-Immunoprecipitation, WB-western blot).

ZNF326 is a novel interaction partner and substrate of the PRMT5/WDR77 complex

As the PRMT5/WDR77 complex showed increased nuclear accumulation in MDA-MB-231 cells, we focused our analysis on the novel nuclear interaction partners of WDR77. Among the top nuclear interaction partners of WDR77 was ZNF326, a 68 kDa zinc finger protein that has been previously characterized to be a part of the DBIRD complex that travels along with core mRNP particle during transcription, regulating splicing by controlling the rate of transcriptional elongation by Pol II (51). Splicing being mainly co-transcriptional (52) we wanted to understand if the PRMT5/WDR77 complex played a previously uncharacterized role in regulating splicing through transcriptional elongation.

To understand if ZNF326 is also overexpressed in breast cancer, we performed qPCR and immunoblotting of nuclear and cytoplasmic extracts of breast cancer cell lines. ZNF326 is overexpressed in ER-breast cancer cell lines (MDA-MB-231 and HCC38) relative to MCF10A cells and showed nuclear localization (Supplementary Figure S2D and E).

To investigate if PRMT5 and WDR77 are components of the core mRNP particle and to validate our mass spectrometry observations, we performed co-immunoprecipitation experiments from nuclear extracts of MDA-MB-231 cells. We confirmed the interaction of ZNF326 with PRMT5 and WDR77. HNRNPH1, a component of the mRNP particle was also observed to interact with the PRMT5/WDR77 complex (Figure 2E).

Substrates of the PRMT5/WDR77 complex including histones and transcription factors are characterized by the presence of glycine-arginine repeats at which they are methylated (10). Interestingly, we identified two RG-rich motifs in ZNF326, at positions 173 (RGRG) and 199 (GRGRGRG), making it a likely substrate of the PRMT5/WDR77 complex (Figure 3A).

We used the SYM10 antibody (53) for immunoblotting to determine if endogenous ZNF326 was symmetrically dimethylated. We confirmed the specificity of the SYM10 antibody to detect symmetrically dimethylated arginines (Supplementary Figure S3A) and used it to immunoblot ZNF326 that was immunoprecipitated from nuclear extracts of MDA-MB-231 and confirmed that the endogenous protein is symmetrically dimethylated (Figure 3B). To identify the arginine residue(s) methylated and to verify if the modification(s) occurred in a PRMT5/WDR77-dependent manner, we immunoprecipitated endogenous ZNF326 from uninfected, sh_scrambled, sh_WDR77 and sh_PRMT5 infected MDA-MB-231 cells and analyzed the samples by LC-MS/MS. We observed that ZNF326 is primarily dimethylated at Arginine 175 (R175) (Figure 3C) and this modification is lost in a PRMT5 and WDR77-dependent manner (Figure 3D and E). To confirm that ZNF326 is a *bona fide* substrate of the PRMT5/WDR77 complex we performed *in vitro* methylation assays. We observed that only the wt ZNF326 peptide and not the mutated ZNF326R175K peptide was methylated by the PRMT5/WDR77 complex (Supplementary Figure S3B).

Loss of PRMT5 and WDR77 results in inclusion of A-T rich exons at target genes

To understand the effect of loss of PRMT5, WDR77 and subsequent loss of ZNF326 methylation on alternative splicing, we performed RNA-seq analysis on *PRMT5* and *WDR77* depleted MDA-MB-231 cells. Gene ontology analysis revealed an upregulation of apoptotic genes upon loss of *PRMT5* and *WDR77* in MDA-MB-231 cells (Supplementary Figure S4A) explaining our earlier observation of an increase in the number of apoptotic cells. Genes involved in RNA processing was observed to be the top category of affected genes revealed by GO analysis of genes that are alternatively spliced upon loss of *PRMT5* and *WDR77* (Supplementary Figure S4B).

As one of the major roles of the PRMT5/WDR77 complex is the symmetric methylation of spliceosome proteins, we evaluated the effect of knockdown of PRMT5 and WDR77 on splicing. Comparison of the RNA-seq datasets revealed that 256 genes are alternatively spliced upon loss of WDR77 and PRMT5. These categories include genes involved in mRNA cleavage and polyadenylation (*CPSF1*, *CPSF7*, *CPSF3L*), splicing (*U2AF1*, *RBM23*, *RBM5*, *HNRNPC*, *HNRNPH1*, *RBM39*), mRNA structure and stability (*DDX23*) and mRNA degradation (*EXOSC9*). mRNA is alternatively spliced through several physical mechanisms including the usage of different 5′ and 3′ splice sites, intron retention or exon inclusion/exclusion (Supplementary Figure S4C). shRNA knockdown of WDR77 and PRMT5 caused defects in constitutive and alternative splicing, primarily through exon skipping (SE) causing altered inclusion or exclusion of exons compared to cells treated with scrambled shRNA control (Supplementary Figure S4D and E). This is in accordance with previously work showing that genes with 5′ weak donor site undergo exon skipping upon knockdown of PRMT5 (15) due to loss of methylation of the spliceosome proteins disrupting the formation of the spliceosome. As ZNF326 has been reported to be essential for transcription across A-T rich regions, we wanted to check if loss of methylation of ZNF326 resulted in altered splicing at A-T rich genes. Interestingly we observed inclusion of A-T rich exons in the WDR77 and PRMT5 knockdown cells (Figure 4A and B) a phenomenon that was observed previously upon knockdown of ZNF326 (51).

A-T rich tracts have been previously reported to be refractory to transcription (54) and this result reinforces the requirement of methylated ZNF326 for normal transcription across this region as loss of PRMT5 or WDR77 does not result in decreased stability/loss of ZNF326 protein (Supplementary Figure S2F).

Alternative splicing coupled mRNA decay upon loss of PRMT5

We then proceeded to evaluate the correlation between genes that were alternatively spliced and genes that were differentially regulated upon knockdown of PRMT5. Scatter plot analysis of genes alternatively spliced upon loss of *PRMT5* or *WDR77* revealed that several of the alternatively spliced genes were differentially regulated (Figure 4C and D). About 11.5% of genes that were alternatively spliced were also downregulated upon loss of *PRMT5*

A

B

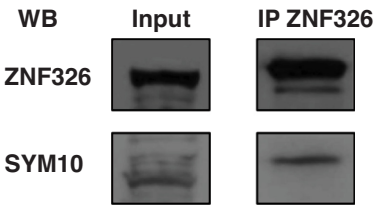

C

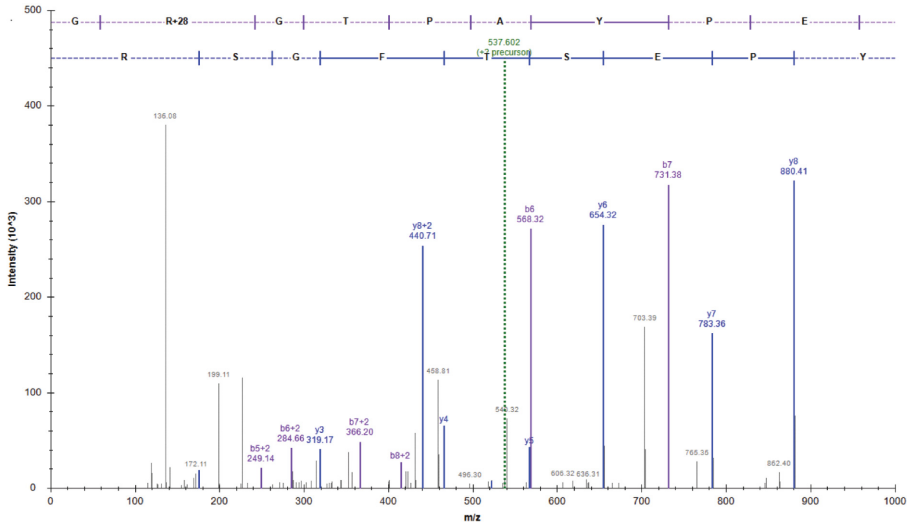

D

Peptide	Relative abundance		
	sh Scrambled	sh WDR77	sh PRMT5
FGGSYGGR	1	0.976466442	1.53881826
FGPYESYDSR	1	1.139379318	1.1125581
NQGGSSWEAPYSR	1	0.803831893	1.252488546
SGYGFNEPEQSR	1	0.947964244	1.167280642
GR[+28]GTPAYPESTFGSR	1	0.11724339	0.009327715
GR[+28]GTPAYPESTFGSR	1	0.188017222	0.000631836

E

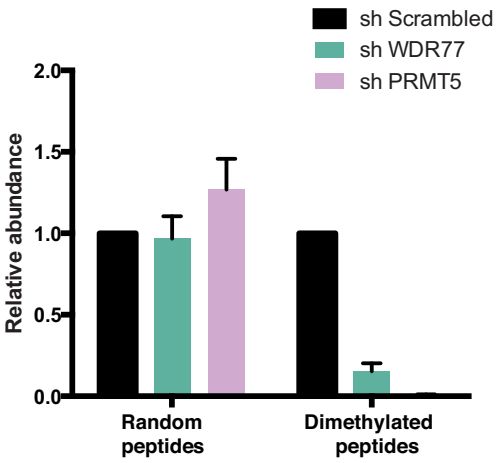

Figure 3. ZNF326 is symmetrically dimethylated at R175 by the PRMT5/WDR77 complex (**A**). ZNF326 has two glycine-arginine rich motifs. Asterisk indicates R175 that was identified to be dimethylated (**B**). Immunoblots of immunoprecipitates showing symmetric dimethylation of ZNF326 (**C**). Representative tandem mass spectrum of the peptide GR(28.0314)GTPAYPESTFGSR {m/z:537.602 (+3). The fragment ion matching within 10 ppm are shown as either the B-ion (purple) or Y-ion (blue) series. The green dashed line indicates precursor m/z. The dotted lines in the fragmentation ladder sequence on the top the spectrum corresponds to the missing B-ion (purple) and Y-ion (blue) series (**D**). Mass Spectrometry analysis showing the relative abundance of random and dimethylated peptides in cells infected with sh Scrambled, sh *WDR77* and sh *PRMT5* and (**E**). Graphical representation of the same.

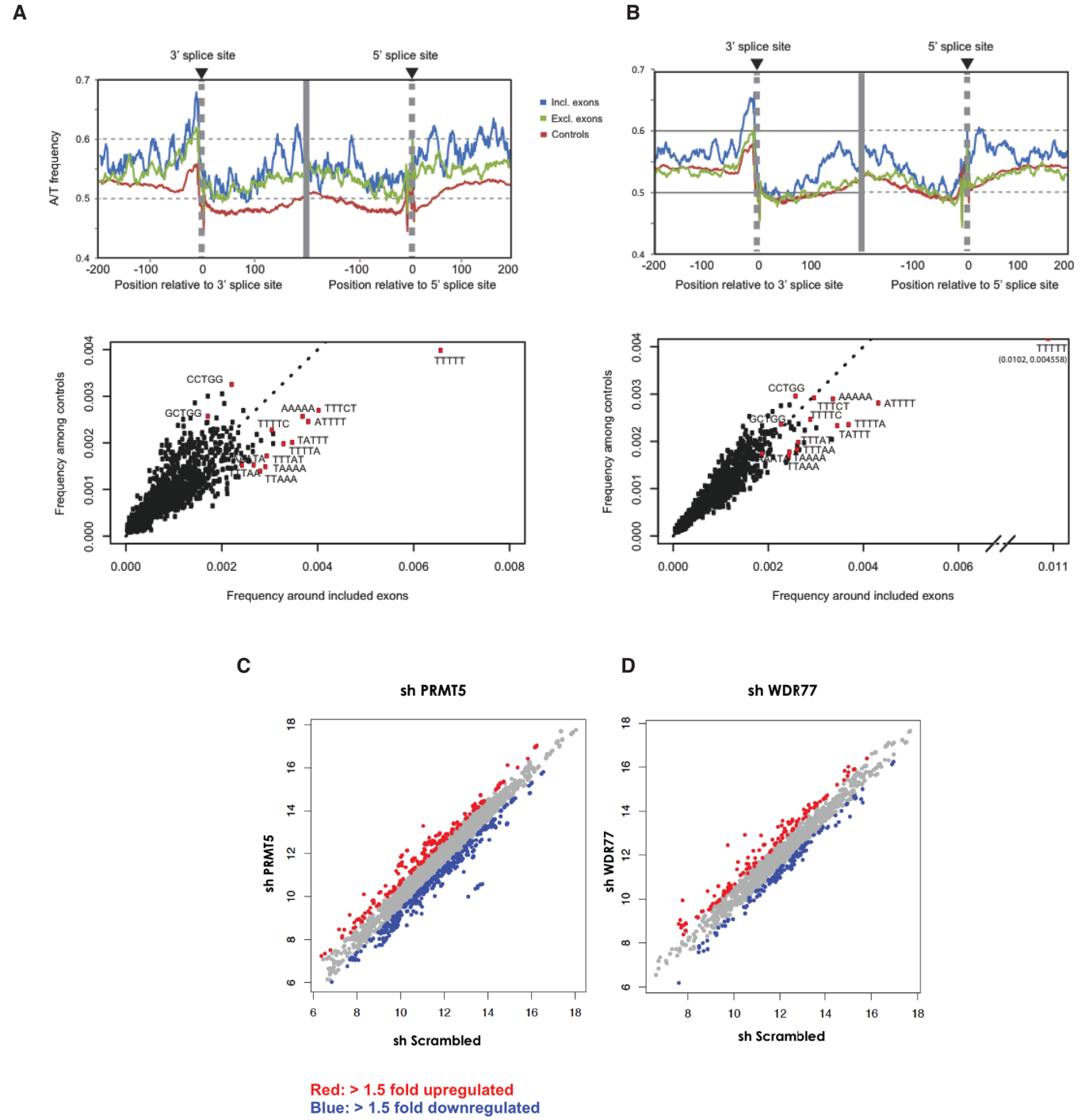

Figure 4. Loss of *PRMT5* and *WDR77* leads to defects in alternative splicing and inclusion of A-T rich exons (**A** and **B**). (Top) Frequency of A or T upstream and downstream from splice sites of included exons (blue) excluded exons (green) and unaffected control exons (red). The dotted black line marks the meeting point of upstream and downstream datasets. (Below) Frequency of 5-base oligonucleotides in the regions around splice sites of included (*x*-axis) versus control (*y*-axis) exons in sh WDR77 (Left) and sh PRMT5 (Right) samples. Scatter plot of genes that are alternatively spliced and up- or downregulated upon loss of WDR77 (**C**) and PRMT5 (**D**) relative to scrambled shRNA control (Red- >1.5-fold upregulated Blue- >1.5-fold downregulated).

suggesting that the alternative splicing of these transcripts could contribute to decreased transcript stability (Supplementary Figure S4F). Furthermore, 64.5% (109 of 169 genes) of these genes that were downregulated were alternatively spliced by inclusion/exclusion of exons (Supplementary Figure S4G).

Interestingly, several genes that were downregulated such as *ST3GAL6* (55), *FOXM1* (56) and *AP4* (57) play a key role in breast cancer tumorigenesis and this interested us to probe more carefully how this regulation was orchestrated by the PRMT5/ WDR77 complex.

We then performed qPCR analysis to investigate if some of these alternatively spliced transcripts were downregulated because of decreased transcript stability. To understand if the downregulation of the transcripts was attributed to alternative splicing and to differentiate it from transcriptional downregulation, it was essential to quantitate pre-mRNA, mRNA and exon levels of the specific transcript. To this end, we designed intron–exon primers (to quantitate pre-mRNA), exon–exon primers (to quantitate mRNA) and intra–exon primers (to quantitate exon levels). All the primers used for RT-PCR are listed in Supplementary Table S4**.**

We tested genes involved in monosaccharide metabolism (*ST3GAL6*, *PFKM*), DNA metabolism (*REPIN1*/*AP4*) and TRNAU1AP/SECP43 that has been implicated in nonsense-mediated decay (58), as these were also the top categories of genes that had alternate exon inclusion and were downregulated upon loss of *PRMT5*. In all these genes, we detected inclusion of the specific exon, no significant difference in the pre-mRNA levels but downregulation of mRNA in sh_PRMT5 relative to control scrambled shRNA infected cells (Figure 5A–D). Exon inclusion for *ST3GAL6*, *REPIN1*/*AP4* and *PFKM* was observed upon loss of WDR77 but the downregulation was not observed in all cases (Supplementary Figure S5A–C). To rule out the possibility that this was just due to reduced stability of mRNA versus pre-mRNA we performed qPCR for a control gene, MED28 (Supplementary Figure S5D) that is not transcriptionally regulated or spliced upon loss of *PRMT5* and did not observe any significant difference relative to control.

DISCUSSION

PRMT5 and *WDR77* are known oncogenes (20,24,41,59) and analysis of METABRIC (Molecular Taxonomy of Breast Cancer International Consortium) data revealed overexpression of PRMT5 correlates to poor survival (Supplementary Figure S6). We chose breast cancer as a model system for two reasons- first, because the PRMT5/WDR77 complex showed increased nuclear accumulation, and second, there is very little known (60) on the intra-nuclear role of the PRMT5/WDR77 complex in regulating splicing.

We shown for the first time the multi-layered regulation of WDR77 by PRMT5, both at the level of mRNA transcript (either through transcriptional or post-transcriptional regulation) and protein. However, RNA-seq analysis revealed that the overlap of genes upregulated upon loss of *WDR77* and *PRMT5* is 12.24 and 27.3% respectively. This could be explained because loss of *PRMT5* leads to the depletion of both proteins and hence showed increased overlap. Moreover, the PRMT5/WDR77 complex is a part of many intracellular complexes including MBD2-NuRD (14) and components of Mediator (61) and loss of either protein would affect target genes depending on its stoichiometry in the complex. Loss of *WDR77* and *PRMT5* reduces cell viability and induces apoptosis in MDA-MB-231 cells. Apoptosis could have been triggered by the upregulation of pro-apoptotic genes including *CASP3* and *IL6* (RNA-seq analysis of sh_WDR77 and sh_PRMT5) and loss of *AP4*, which is alternatively spliced and subjected to decay upon loss of PRMT5 (62,63).

To identify novel interaction partners that could possibly be mediators of breast cancer oncogenesis along with PRMT5/WDR77 complex, we performed the first comprehensive characterization of the nuclear and cytoplasmic interaction partners of endogenous WDR77.

We identified novel interaction partners involved in the regulation of all the major steps of gene expression ranging from transcription (Rbbp4, Rbbp7, FUBP1), mRNA stability (SERBP1) and processing (LARP1, FUBP2), splicing (HNRNPH1 and H2, ZNF326), mRNA export (CAPRIN1, G3BP1) and translation (RPS10, RPS26). Association of hnRNPH1 (and hnRNPs H2, H3, F, R, A1 among others) with PRMT5 brings in a new factor that could possibly govern the sub-cellular localization and/or activity of these hnRNPs that were previously only known to be asymmetrically dimethylated.

The trio of PRMT5, WDR77 and ZNF326 are known to regulate alternative splicing; the PRMT5/WDR77 complex is involved in symmetric dimethylation of spliceosome proteins (7) while ZNF326 interacts with Pol II and HNRNPs and regulates the rate of transcriptional elongation across AT-rich regions (51).

ZNF326 belongs to the AKAP95 family of proteins (which includes ZNF326, AKAP95 and HA95) (64,65)**.** AKAP95 has also been shown to interact with HNRNP-H1 along with HNRNPs F and M; however unlike ZNF326, loss of AKAP95 promotes exon skipping (51,64).

We have shown that ZNF326 is a substrate of the PRMT5/WDR77 complex, and that loss of ZNF326 methylation, mimics loss of ZNF326 (51) and leads to alternative splicing of target genes by the inclusion of A-T rich exons.

Around 11.5% of genes that are alternatively spliced upon loss of PRMT5 are downregulated suggesting that the alternative splicing could contribute to transcript destabilization and decay. Several of the alternatively spliced and downregulated genes identified play an important role in oncogenesis and metastasis, including *ST3GAL6* which is essential for homing and survival in multiple myeloma (66) and is a marker for metastasis in breast cancer (55), *PFKM* which has been identified as a novel breast cancer gene by a genome-wide association study (67) and *AP4* (68) which is associated with promoting oncogenesis and poor survival in several types of cancer (68,69) and was recently described as the driver of EMT in MDA-MB-231 cells (70).

Predictions from studies of mouse and human EST data suggest that one-fifth of alternatively spliced mouse and human genes produce premature termination containing (PTC) RNAs that could be subject to nonsense mediated

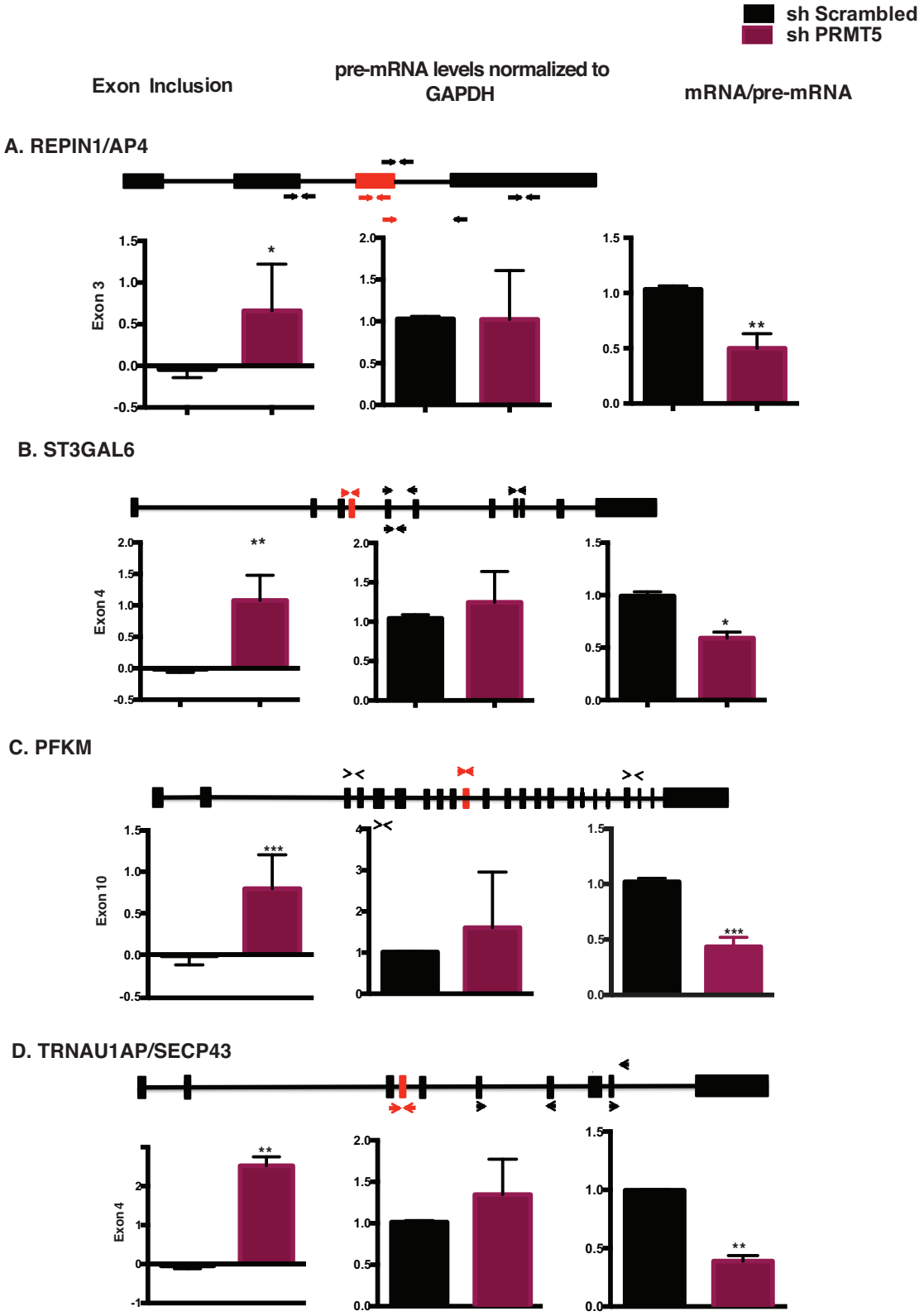

Figure 5. Alternative splicing coupled mRNA decay of transcripts upon loss of *PRMT5*. qPCR analysis showing (from left to right) relative levels of exon inclusion, pre-mRNA and the mRNA/pre-mRNA ratio in sh Scrambled and sh *PRMT5* samples for (**A**) *REPIN1/AP4* (**B**) *ST3GAL6* (**C**) *PFKM* (**D**) *TRNAU1AP/SECP43*. The illustrations depict the gene structure with exons shown as black boxes and introns as lines. The included exons are shown in red. Arrows indicate regions to which primers were designed. Student's *t*-test $*P < 0.05$ $**P < 0.005$ $***P < 0.0005$.

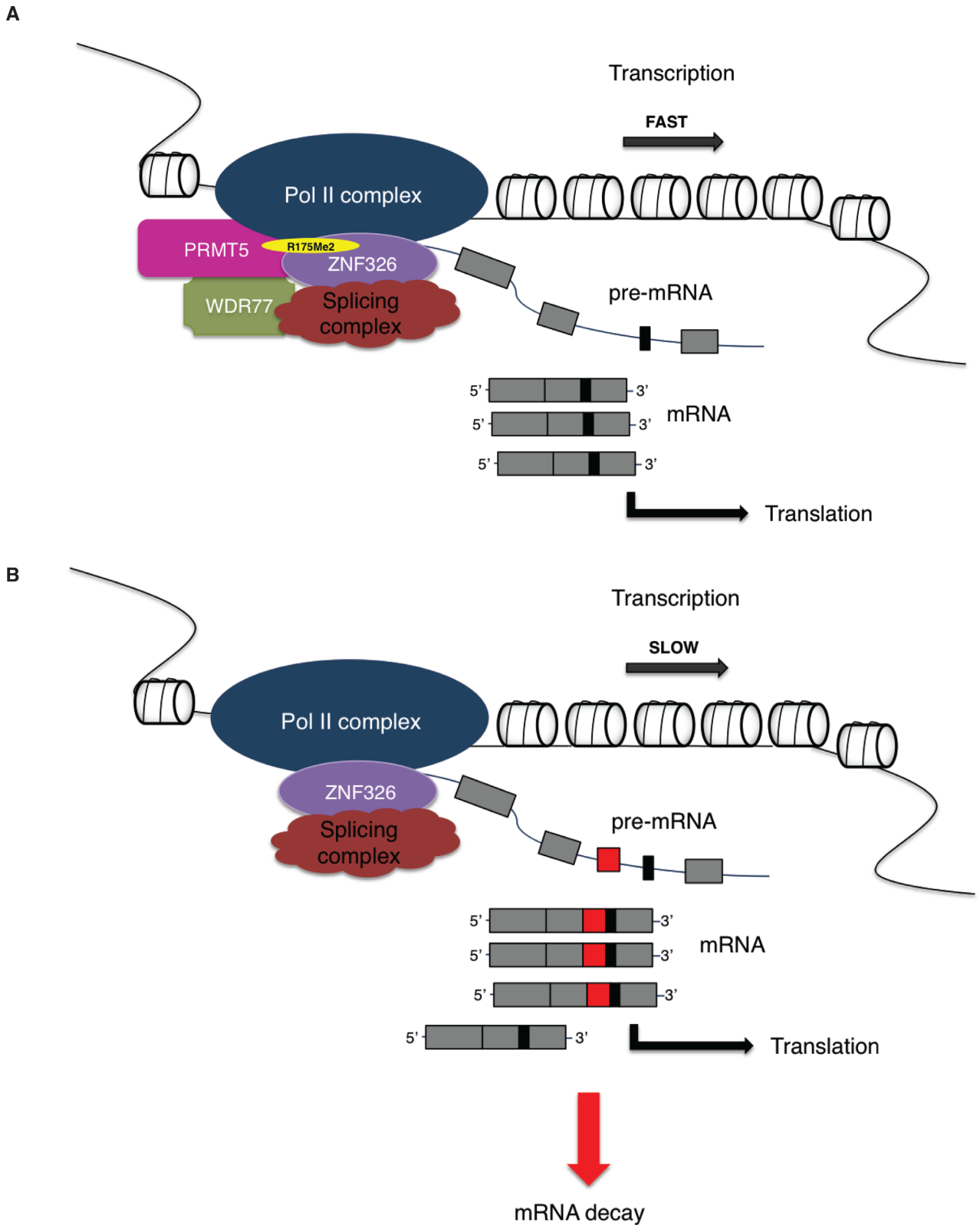

Figure 6. The PRMT5/WDR77 complex shapes the transcriptome of MDA-MB-231 cells through methylation of ZNF326. Methylation of ZNF326 by the PRMT5/WDR77 complex is essential for Pol II transcription across A-T rich genes. Loss of *PRMT5* or *WDR77* leads to a loss of methylation of ZNF326 that results in slow progression of Pol II causing the inclusion of A-T rich exons in target genes. A subset of these transcripts is targeted for degradation thereby altering the shape of the transcriptome of the cell. (**A**) Represents the influence of PRMT5/WDR77 to coordinate the rate at which transcription may help determine splicing patterns, where, the absence of PRMT5/WDR77 (**B**) effects the rate and aberrant inclusion of exons.

decay (71). It is likely that a majority of these transcripts are a result of transcriptional and splicing noise and that the surveillance is just a housekeeping mechanism. However looking through our analysis there are several intriguing links that cannot be ignored. The loss of methylation of ZNF326 leading to alternate inclusion of A-T rich exons and the downregulation of genes that have been previously identified as drivers of cancer progression point to a nuanced mechanism of gene expression regulation.

Recently, Zhao *et. al* (72) published the symmetric dimethylation of Pol II by PRMT5 and regulation of transcription termination. As PRMT5/WDR77 complex also methylates FCP1 (73) and SPT5 (60) and ZNF326 the multi-pronged control exerted by this complex in transcription and splicing requires further investigation.

To summarize, we have identified a novel role played by the intra-nuclear PRMT5/WDR77 complex in regulating splicing and breast cancer oncogenesis. Through this paper we have two new findings: (i) ZNF326 (a component of the mRNP particle) is a newly identified bona fide substrate of PRMT5 and (ii) loss of methylation of ZNF326 leads to inclusion of A-T rich exons, a phenomenon that has been observed upon loss of ZNF326 by other researchers (51).

It seems likely that methylation of ZNF326 is essential for the transcription of Pol II across A-T rich genes. Loss of *WDR77* and *PRMT5* results in loss of methylation of ZNF326 and resulted in the inclusion of A-T rich exons in target genes (Figure 6). A subset of genes that undergo alternative inclusion of exons are unstable and are downregulated (possibly through downstream mechanisms such as nonsense-mediated decay). Our data, thereby, supports the role of the PRMT5/WDR77 complex in shaping the breast cancer transcriptome by fine-tuning the balance between splicing and stability.

ACCESSION NUMBER

Gene Expression Omnibus (GEO) GSE75741.

SUPPLEMENTARY DATA

Supplementary Data are available at NAR Online.

ACKNOWLEDGEMENTS

We thank Dr Alicia Alonso and Yushan Li of the Weill-Cornell College of Medicine's Epigenomic Sequencing Core for expert advice and support for sequencing and library preparation for RNA-seq. We also acknowledge Chih-Hung Chen for technical assistance.

FUNDING

Ellison Medical Foundation Senior Scholar Award in Aging [AG-SS-2482–10 to M.J.W.]; National Institutes of Health [5RO1HL103967, 5RO1CA154903, to M.J.W., 5RO1GM089778 to J.A.W.]. Funding for open access charge: NIH.
Conflict of interest statement. None declared.

REFERENCES

1. Di Lorenzo,A. and Bedford,M.T. (2011) Histone arginine methylation. *FEBS Lett.*, **585**, 2024–2031.
2. Bedford,M.T. and Richard,S. (2005) Arginine methylation an emerging regulator of protein function. *Mol. Cell*, **18**, 263–272.
3. Bedford,M.T. and Clarke,S.G. (2009) Protein arginine methylation in mammals: who, what, and why. *Mol. Cell*, **33**, 1–13.
4. Yang,Y., Hadjikyriacou,A., Xia,Z., Gayatri,S., Kim,D., Zurita-Lopez,C., Kelly,R., Guo,A., Li,W., Clarke,S.G. *et al.* (2015) PRMT9 is a type II methyltransferase that methylates the splicing factor SAP145. *Nat. Commun.*, **6**, 6428.
5. Antonysamy,S., Bonday,Z., Campbell,R.M., Doyle,B., Druzina,Z., Gheyi,T., Han,B., Jungheim,L.N., Qian,Y., Rauch,C. *et al.* (2012) Crystal structure of the human PRMT5:MEP50 complex. *Proc. Natl. Acad. Sci. U.S.A.*, **109**, 17960–17965.
6. Ho,M.C., Wilczek,C., Bonanno,J.B., Xing,L., Seznec,J., Matsui,T., Carter,L.G., Onikubo,T., Kumar,P.R., Chan,M.K. *et al.* (2013) Structure of the arginine methyltransferase PRMT5-MEP50 reveals a mechanism for substrate specificity. *PLoS One*, **8**, e57008.
7. Friesen,W.J., Wyce,A., Paushkin,S., Abel,L., Rappsilber,J., Mann,M. and Dreyfuss,G. (2002) A novel WD repeat protein component of the methylosome binds Sm proteins. *J. Biol. Chem.*, **277**, 8243–8247.
8. Tabata,T., Kokura,K., Ten Dijke,P. and Ishii,S. (2009) Ski co-repressor complexes maintain the basal repressed state of the TGF-beta target gene, SMAD7, via HDAC3 and PRMT5. *Genes Cells*, **14**, 17–28.
9. Migliori,V., Muller,J., Phalke,S., Low,D., Bezzi,M., Mok,W.C., Sahu,S.K., Gunaratne,J., Capasso,P., Bassi,C. *et al.* (2012) Symmetric dimethylation of H3R2 is a newly identified histone mark that supports euchromatin maintenance. *Nat. Mol. Biol.*, **19**, 136–144.
10. Jansson,M., Durant,S.T., Cho,E.C., Sheahan,S., Edelmann,M., Kessler,B. and La Thangue,N.B. (2008) Arginine methylation regulates the p53 response. *Nat. Cell Biol.*, **10**, 1431–1439.
11. Cho,E.C., Zheng,S., Munro,S., Liu,G., Carr,S.M., Moehlenbrink,J., Lu,Y.C., Stimson,L., Khan,O., Konietzny,R. *et al.* (2012) Arginine methylation controls growth regulation by E2F-1. *EMBO J.*, **31**, 1785–1797.
12. Wei,H., Wang,B., Miyagi,M., She,Y., Gopalan,B., Huang,D.B., Ghosh,G., Stark,G.R. and Lu,T. (2013) PRMT5 dimethylates R30 of the p65 subunit to activate NF-kappaB. *Proc. Natl. Acad. Sci. U.S.A.*, **110**, 13516–13521.
13. Stopa,N., Krebs,J.E. and Shechter,D. (2015) The PRMT5 arginine methyltransferase: many roles in development, cancer and beyond. *Cell. Mol. Life Sci.*, **72**, 2041–2059.
14. Le Guezennec,X., Vermeulen,M., Brinkman,A.B., Hoeijmakers,W.A., Cohen,A., Lasonder,E. and Stunnenberg,H.G. (2006) MBD2/NuRD and MBD3/NuRD, two distinct complexes with different biochemical and functional properties. *Mol. Cell. Biol.*, **26**, 843–851.
15. Bezzi,M., Teo,S.X., Muller,J., Mok,W.C., Sahu,S.K., Vardy,L.A., Bonday,Z.Q. and Guccione,E. (2013) Regulation of constitutive and alternative splicing by PRMT5 reveals a role for Mdm4 pre-mRNA in sensing defects in the spliceosomal machinery. *Genes Dev.*, **27**, 1903–1916.
16. Koh,C.M., Bezzi,M., Low,D.H., Ang,W.X., Teo,S.X., Gay,F.P., Al-Haddawi,M., Tan,S.Y., Osato,M., Sabo,A. *et al.* (2015) MYC regulates the core pre-mRNA splicing machinery as an essential step in lymphomagenesis. *Nature* , **523**, 96–100.
17. Sanchez,S.E., Petrillo,E., Beckwith,E.J., Zhang,X., Rugnone,M.L., Hernando,C.E., Cuevas,J.C., Godoy Herz,M.A., Depetris-Chauvin,A., Simpson,C.G. *et al.* (2010) A methyl transferase links the circadian clock to the regulation of alternative splicing. *Nature*, **468**, 112–116.
18. Hong,S., Song,H.R., Lutz,K., Kerstetter,R.A., Michael,T.P. and McClung,C.R. (2010) Type II protein arginine methyltransferase 5 (PRMT5) is required for circadian period determination in Arabidopsis thaliana. *Proc. Natl. Acad. Sci. U.S.A.*, **107**, 21211–21216.
19. Ibrahim,R., Matsubara,D., Osman,W., Morikawa,T., Goto,A., Morita,S., Ishikawa,S., Aburatani,H., Takai,D., Nakajima,J. *et al.* (2014) Expression of PRMT5 in lung adenocarcinoma and its significance in epithelial-mesenchymal transition. *Hum. Pathol.*, **45**, 1397–1405.

20. Han,X., Li,R., Zhang,W., Yang,X., Wheeler,C.G., Friedman,G.K., Province,P., Ding,Q., You,Z., Fathallah-Shaykh,H.M. *et al.* (2014) Expression of PRMT5 correlates with malignant grade in gliomas and plays a pivotal role in tumor growth in vitro. *J. neuro-oncol.*, **118**, 61–72.
21. Pal,S., Baiocchi,R.A., Byrd,J.C., Grever,M.R., Jacob,S.T. and Sif,S. (2007) Low levels of miR-92b/96 induce PRMT5 translation and H3R8/H4R3 methylation in mantle cell lymphoma. *EMBO J.*, **26**, 3558–3569.
22. Zhang,H.T., Zhang,D., Zha,Z.G. and Hu,C.D. (2014) Transcriptional activation of PRMT5 by NF-Y is required for cell growth and negatively regulated by the PKC/c-Fos signaling in prostate cancer cells. *Biochim. Biophys. Acta*, **1839**, 1330–1340.
23. Ligr,M., Patwa,R.R., Daniels,G., Pan,L., Wu,X., Li,Y., Tian,L., Wang,Z., Xu,R., Wu,J. *et al.* (2011) Expression and function of androgen receptor coactivator p44/Mep50/WDR77 in ovarian cancer. *PLoS One*, **6**, e26250.
24. Peng,Y., Li,Y., Gellert,L.L., Zou,X., Wang,J., Singh,B., Xu,R., Chiriboga,L., Daniels,G., Pan,R. *et al.* (2010) Androgen receptor coactivator p44/Mep50 in breast cancer growth and invasion. *J. Cell. Mol. Med.*, **14**, 2780–2789.
25. Kaiser,P. and Wohlschlegel,J. (2005) Identification of ubiquitination sites and determination of ubiquitin-chain architectures by mass spectrometry. *Methods Enzymol.*, **399**, 266–277.
26. Wohlschlegel,J.A. (2009) Identification of SUMO-conjugated proteins and their SUMO attachment sites using proteomic mass spectrometry. *Methods Mol. Biol.*, **497**, 33–49.
27. Kelstrup,C.D., Young,C., Lavallee,R., Nielsen,M.L. and Olsen,J.V. (2012) Optimized fast and sensitive acquisition methods for shotgun proteomics on a quadrupole orbitrap mass spectrometer. *J. Proteome Res.*, **11**, 3487–3497.
28. Michalski,A., Damoc,E., Hauschild,J.P., Lange,O., Wieghaus,A., Makarov,A., Nagaraj,N., Cox,J., Mann,M. and Horning,S. (2011) Mass spectrometry-based proteomics using Q Exactive, a high-performance benchtop quadrupole Orbitrap mass spectrometer. *Mol. Cell Proteomics*, **10**, doi:10.1074/mcp.M111.011015.
29. Beausoleil,S.A., Villen,J., Gerber,S.A., Rush,J. and Gygi,S.P. (2006) A probability-based approach for high-throughput protein phosphorylation analysis and site localization. *Nat. Biotechnol.*, **24**, 1285–1292.
30. Cociorva,D., D,L.T. and Yates,J.R. (2007) Validation of tandem mass spectrometry database search results using DTASelect. *Curr. Protoc. Bioinformatics*, **16**, doi:10.1002/0471250953.bi1304s16.
31. Tabb,D.L., McDonald,W.H. and Yates,J.R. III (2002) DTASelect and Contrast: tools for assembling and comparing protein identifications from shotgun proteomics. *J. Proteome Res.*, **1**, 21–26.
32. Xu,T., Venable,J.D., Park,S.K., Cociorva,D., Lu,B., Liao,L., Wohlschlegel,J., Hewel,J. and Yates,J.R. III (2006) ProLuCID, a fast and sensitive tandem mass spectra-based protein identification programs. *Mol. Cell. Proteomics*, **5**, S174.
33. Elias,J.E. and Gygi,S.P. (2007) Target-decoy search strategy for increased confidence in large-scale protein identifications by mass spectrometry. *Nat. Methods*, **4**, 207–214.
34. Florens,L., Carozza,M.J., Swanson,S.K., Fournier,M., Coleman,M.K., Workman,J.L. and Washburn,M.P. (2006) Analyzing chromatin remodeling complexes using shotgun proteomics and normalized spectral abundance factors. *Methods*, **40**, 303–311.
35. MacLean,B., Tomazela,D.M., Shulman,N., Chambers,M., Finney,G.L., Frewen,B., Kern,R., Tabb,D.L., Liebler,D.C. and MacCoss,M.J. (2010) Skyline: an open source document editor for creating and analyzing targeted proteomics experiments. *Bioinformatics*, **26**, 966–968.
36. Schilling,B., Rardin,M.J., MacLean,B.X., Zawadzka,A.M., Frewen,B.E., Cusack,M.P., Sorensen,D.J., Bereman,M.S., Jing,E., Wu,C.C. *et al.* (2012) Platform-independent and label-free quantitation of proteomic data using MS1 extracted ion chromatograms in skyline: application to protein acetylation and phosphorylation. *Mol. Cell. Proteomics*, **11**, 202–214.
37. Li,H. and Durbin,R. (2010) Fast and accurate long-read alignment with Burrows-Wheeler transform. *Bioinformatics*, **26**, 589–595.
38. Wang,L., Feng,Z., Wang,X. and Zhang,X. (2010) DEGseq: an R package for identifying differentially expressed genes from RNA-seq data. *Bioinformatics*, **26**, 136–138.
39. Huang da,W., Sherman,B.T. and Lempicki,R.A. (2009) Bioinformatics enrichment tools: paths toward the comprehensive functional analysis of large gene lists. *Nucleic Acids Res.*, **37**, 1–13.
40. Huang da,W., Sherman,B.T. and Lempicki,R.A. (2009) Systematic and integrative analysis of large gene lists using DAVID bioinformatics resources. *Nat. Protoc.*, **4**, 44–57.
41. Peng,Y., Chen,F., Melamed,J., Chiriboga,L., Wei,J., Kong,X., McLeod,M., Li,Y., Li,C.X., Feng,A. *et al.* (2008) Distinct nuclear and cytoplasmic functions of androgen receptor cofactor p44 and association with androgen-independent prostate cancer. *Proc. Natl. Acad. Sci. U.S.A.*, **105**, 5236–5241.
42. He,H.H., Meyer,C.A., Chen,M.W., Jordan,V.C., Brown,M. and Liu,X.S. (2012) Differential DNase I hypersensitivity reveals factor-dependent chromatin dynamics. *Genome Res.*, **22**, 1015–1025.
43. Hah,N., Murakami,S., Nagari,A., Danko,C.G. and Kraus,W.L. (2013) Enhancer transcripts mark active estrogen receptor binding sites. *Genome Res.*, **23**, 1210–1223.
44. Ho,M.C., Wilczek,C., Bonanno,J.B., Xing,L., Seznec,J., Matsui,T., Carter,L.G., Onikubo,T., Kumar,P.R., Chan,M.K. *et al.* (2013) Structure of the arginine methyltransferase PRMT5-MEP50 reveals a mechanism for substrate specificity. *PLoS One*, **8**, e57008.
45. Gonsalvez,G.B., Tian,L., Ospina,J.K., Boisvert,F.M., Lamond,A.I. and Matera,A.G. (2007) Two distinct arginine methyltransferases are required for biogenesis of Sm-class ribonucleoproteins. *J. Cell Biol.*, **178**, 733–740.
46. Gkountela,S., Li,Z., Chin,C.J., Lee,S.A. and Clark,A.T. (2014) PRMT5 is required for human embryonic stem cell proliferation but not pluripotency. *Stem Cell Rev.*, **10**, 230–239.
47. Scoumanne,A., Zhang,J. and Chen,X. (2009) PRMT5 is required for cell-cycle progression and p53 tumor suppressor function. *Nucleic Acids Res.*, **37**, 4965–4976.
48. Wilczek,C., Chitta,R., Woo,E., Shabanowitz,J., Chait,B.T., Hunt,D.F. and Shechter,D. (2011) Protein arginine methyltransferase Prmt5-Mep50 methylates histones H2A and H4 and the histone chaperone nucleoplasmin in Xenopus laevis eggs. *J. Biol. Chem.*, **286**, 42221–42231.
49. Aggarwal,P., Vaites,L.P., Kim,J.K., Mellert,H., Gurung,B., Nakagawa,H., Herlyn,M., Hua,X., Rustgi,A.K., McMahon,S.B. *et al.* (2010) Nuclear cyclin D1/CDK4 kinase regulates CUL4 expression and triggers neoplastic growth via activation of the PRMT5 methyltransferase. *Cancer Cell*, **18**, 329–340.
50. Guderian,G., Peter,C., Wiesner,J., Sickmann,A., Schulze-Osthoff,K., Fischer,U. and Grimmler,M. (2011) RioK1, a new interactor of protein arginine methyltransferase 5 (PRMT5), competes with pICln for binding and modulates PRMT5 complex composition and substrate specificity. *J. Biol. Chem.*, **286**, 1976–1986.
51. Close,P., East,P., Dirac-Svejstrup,A.B., Hartmann,H., Heron,M., Maslen,S., Chariot,A., Soding,J., Skehel,M. and Svejstrup,J.Q. (2012) DBIRD complex integrates alternative mRNA splicing with RNA polymerase II transcript elongation. *Nature*, **484**, 386–389.
52. Tilgner,H., Knowles,D.G., Johnson,R., Davis,C.A., Chakrabortty,S., Djebali,S., Curado,J., Snyder,M., Gingeras,T.R. and Guigo,R. (2012) Deep sequencing of subcellular RNA fractions shows splicing to be predominantly co-transcriptional in the human genome but inefficient for lncRNAs. *Genome Res.*, **22**, 1616–1625.
53. Boisvert,F.M., Cote,J., Boulanger,M.C., Cleroux,P., Bachand,F., Autexier,C. and Richard,S. (2002) Symmetrical dimethylarginine methylation is required for the localization of SMN in Cajal bodies and pre-mRNA splicing. *J. Cell Biol.*, **159**, 957–969.
54. Sigurdsson,S., Dirac-Svejstrup,A.B. and Svejstrup,J.Q. (2010) Evidence that transcript cleavage is essential for RNA polymerase II transcription and cell viability. *Mol. Cell*, **38**, 202–210.
55. Milde-Langosch,K., Karn,T., Schmidt,M., zu Eulenburg,C., Oliveira-Ferrer,L., Wirtz,R.M., Schumacher,U., Witzel,I., Schutze,D. and Muller,V. (2014) Prognostic relevance of glycosylation-associated genes in breast cancer. *Breast Cancer Res. Treat.*, **145**, 295–305.
56. Yu,G., Zhou,A., Xue,J., Huang,C., Zhang,X., Kang,S.H., Chiu,W.T., Tan,C., Xie,K., Wang,J. *et al.* (2015) FoxM1 promotes breast tumorigenesis by activating PDGF-A and forming a positive feedback loop with the PDGF/AKT signaling pathway. *Oncotarget*, **6**, 11281–11294.
57. Chen,S. and Chiu,S.K. (2015) AP4 activates cell migration and EMT mediated by p53 in MDA-MB-231 breast carcinoma cells. *Mol. Cell. Biochem.*, **407**, 57–68.

58. Small-Howard,A., Morozova,N., Stoytcheva,Z., Forry,E.P., Mansell,J.B., Harney,J.W., Carlson,B.A., Xu,X.M., Hatfield,D.L. and Berry,M.J. (2006) Supramolecular complexes mediate selenocysteine incorporation in vivo. *Mol. Cell. Biol.*, **26**, 2337–2346.
59. Yi,P., Gao,S., Gu,Z., Huang,T. and Wang,Z. (2014) P44/WDR77 restricts the sensitivity of proliferating cells to TGFbeta signaling. *Biochem. Biophys. Res. Commun.*, **450**, 409–415.
60. Kwak,Y.T., Guo,J., Prajapati,S., Park,K.J., Surabhi,R.M., Miller,B., Gehrig,P. and Gaynor,R.B. (2003) Methylation of SPT5 regulates its interaction with RNA polymerase II and transcriptional elongation properties. *Mol. Cell*, **11**, 1055–1066.
61. Tsutsui,T., Fukasawa,R., Shinmyouzu,K., Nakagawa,R., Tobe,K., Tanaka,A. and Ohkuma,Y. (2013) Mediator complex recruits epigenetic regulators via its two cyclin-dependent kinase subunits to repress transcription of immune response genes. *J. Biol. Chem.*, **288**, 20955–20965.
62. Liu,X., Zhang,B., Guo,Y., Liang,Q., Wu,C., Wu,L., Tao,K., Wang,G. and Chen,J. (2012) Down-regulation of AP-4 inhibits proliferation, induces cell cycle arrest and promotes apoptosis in human gastric cancer cells. *PLoS One*, **7**, e37096.
63. Jiang,L., Wang,P., Chen,L. and Chen,H. (2014) Down-regulation of FoxM1 by thiostrepton or small interfering RNA inhibits proliferation, transformation ability and angiogenesis, and induces apoptosis of nasopharyngeal carcinoma cells. *Int. J. Clin. Exp. Pathol.*, **7**, 5450–5460.
64. Hu,J., Khodadadi-Jamayran,A., Mao,M., Shah,K., Yang,Z., Nasim,M.T., Wang,Z. and Jiang,H. (2016) AKAP95 regulates splicing through scaffolding RNAs and RNA processing factors. *Nat. Commun.*, **7**, 13347.
65. Castello,A., Fischer,B., Eichelbaum,K., Horos,R., Beckmann,B.M., Strein,C., Davey,N.E., Humphreys,D.T., Preiss,T., Steinmetz,L.M. *et al.* (2012) Insights into RNA biology from an atlas of mammalian mRNA-binding proteins. *Cell*, **149**, 1393–1406.
66. Glavey,S.V., Manier,S., Natoni,A., Sacco,A., Moschetta,M., Reagan,M.R., Murillo,L.S., Sahin,I., Wu,P., Mishima,Y. *et al.* (2014) The sialyltransferase ST3GAL6 influences homing and survival in multiple myeloma. *Blood*, **124**, 1765–1776.
67. Ahsan,H., Halpern,J., Kibriya,M.G., Pierce,B.L., Tong,L., Gamazon,E., McGuire,V., Felberg,A., Shi,J., Jasmine,F. *et al.* (2014) A genome-wide association study of early-onset breast cancer identifies PFKM as a novel breast cancer gene and supports a common genetic spectrum for breast cancer at any age. *Cancer Epidemiol. Biomarkers Prev.*, **23**, 658–669.
68. Shi,L., Jackstadt,R., Siemens,H., Li,H., Kirchner,T. and Hermeking,H. (2014) p53-induced miR-15a/16-1 and AP4 form a double-negative feedback loop to regulate epithelial-mesenchymal transition and metastasis in colorectal cancer. *Cancer Res.*, **74**, 532–542.
69. Gong,H., Han,S., Yao,H., Zhao,H. and Wang,Y. (2014) AP4 predicts poor prognosis in nonsmall cell lung cancer. *Mol. Med. Rep.,* **10**, 336–340.
70. Chen,S. and Chiu,S.K. (2015) AP4 activates cell migration and EMT mediated by p53 in MDA-MB-231 breast carcinoma cells. *Mol. Cell. Biochem.*, **407**, 57–68.
71. Baek,D. and Green,P. (2005) Sequence conservation, relative isoform frequencies, and nonsense-mediated decay in evolutionarily conserved alternative splicing. *Proc. Natl. Acad. Sci. U.S.A.*, **102**, 12813–12818.
72. Yanling Zhao,D., Gish,G., Braunschweig,U., Li,Y., Ni,Z., Schmitges,F.W., Zhong,G., Liu,K., Li,W., Moffat,J. *et al.* (2015) SMN and symmetric arginine dimethylation of RNA polymerase II C-terminal domain control termination. *Nature*, **529**, 48–53.
73. Amente,S., Napolitano,G., Licciardo,P., Monti,M., Pucci,P., Lania,L. and Majello,B. (2005) Identification of proteins interacting with the RNAPII FCP1 phosphatase: FCP1 forms a complex with arginine methyltransferase PRMT5 and it is a substrate for PRMT5-mediated methylation. *FEBS Lett.*, **579**, 683–689.